

NOAA Technical Memorandum ERL PMEL-83

FORMULAS FOR VELOCITY, SEDIMENT CONCENTRATION AND SUSPENDED  
SEDIMENT FLUX FOR STEADY UNI-DIRECTIONAL PRESSURE-DRIVEN FLOW

Harold O. Mofjeld  
J. William Lavelle

Pacific Marine Environmental Laboratory  
Seattle, Washington  
August 1988



**UNITED STATES  
DEPARTMENT OF COMMERCE**

**C. William Verity  
Secretary**

**NATIONAL OCEANIC AND  
ATMOSPHERIC ADMINISTRATION**

**William E. Evans  
Under Secretary for Oceans  
and Atmosphere/Administrator**

**Environmental Research  
Laboratories**

**Vernon E. Derr,  
Director**

## NOTICE

Mention of a commercial company or product does not constitute an endorsement by NOAA/ERL. Use of information from this publication concerning proprietary products or the tests of such products for publicity or advertising purposes is not authorized.

Contribution No. 845 from NOAA/Pacific Marine Environmental Laboratory

---

For sale by the National Technical Information Service, 5285 Port Royal Road  
Springfield, VA 22161

## CONTENTS

PAGE

1.	INTRODUCTION . . . . .	1
2.	STRESS . . . . .	3
3.	EDDY VISCOSITY . . . . .	3
4.	VELOCITY . . . . .	7
5.	SUSPENDED SEDIMENT . . . . .	.10
6.	SUSPENDED SEDIMENT FLUX . . . . .	.14
	A. Slow Settling Velocity (or High Bed Stress) $\beta < 1$ . . . . .	.14
	B. Fast Settling Velocity (or Low Bed Stress) $\beta \geq 2$ . . . . .	.20
	C. Transitional Settling Velocity $1 \leq \beta < 2$ . . . . .	.20
	D. General Dependence of $F/EH$ on $\beta$ and $z_o/H$ . . . . .	.23
7.	CONCLUSIONS . . . . .	.23
8.	ACKNOWLEDGMENTS . . . . .	.23
9.	REFERENCES . . . . .	.25



# Formulas for Velocity, Sediment Concentration and Suspended Sediment Flux for Steady Uni-Directional Pressure-Driven Flow

Harold O. Mofjeld and J. William Lavelle

**ABSTRACT.** A level 2 turbulence closure model for steady pressure-driven currents and suspended sediment concentrations in an unstratified channel leads to analytic formulas for the velocity and the concentration of each settling constituent. The level 2 model uses a parabolic form for the mixing length that increases linearly upward near the bottom and is a maximum at the surface. The model assumes a balance between local turbulence production and dissipation, and the sediment concentrations are assumed to be dilute. The level 2 velocity is found to follow closely the log velocity profile, being only  $\sim 0.5u_*$  less than the log-profile at the surface, where  $u_*$  is the friction velocity (square root of the kinematic bottom stress). The level 2 concentration matches closely a modified form of the Rouse formula in which the actual depth  $H$  is replaced by  $H' = 1.07 H$ . The model results provide a theoretical basis for the use of the log velocity and Rouse concentration profiles over the water column based on turbulence closure theory.

The vertically integrated flux of suspended sediment (suspended load transport) per unit width computed numerically from the level 2 model are approximated well by the flux derived from the pure log velocity and unmodified ( $H' = H$ ) Rouse concentration profiles. When normalized by the ratio of erosion rate to the settling velocity  $w_s$ , explicit formulas for the log-Rouse flux are functions of the two parameters  $\beta = w_s/\kappa u_*$  and  $z_o/H$  ( $\kappa$  being the von Kármán constant,  $z_o$  the bottom roughness and  $H$  the water depth) and is most sensitive to  $\beta$ ; it is proportional to  $\beta^{-1}$  in the slow settling regime  $\beta < 0.1$  and decreasing rapidly as  $\beta^{-1}(\beta-1)^{-2}$  in the fast settling regime  $\beta > 2$ . The flux is a strong function of the bottom stress through the erosion rate which dominates the stress dependence in the slow settling regime.

## 1. INTRODUCTION

In some marine settings the response times of the currents and suspended sediment are sufficiently short compared with the time scales of the forcing that a quasi-steady equilibrium is established between the processes which determines the current and sediment profiles in the water column. In frictionally dominated systems such as shallow nearshore regions, shallow estuarine channels and rivers, the steady current profile is largely the result of a balance between forcing and frictional stress. This stress is often modeled as the product of the current shear and an eddy viscosity which is due in turn to the production of turbulence by the shear. When the concentrations of each settling constituent is sufficiently dilute, its steady concentration profile is the result of a balance between upward turbulent diffusion and downward settling in the water column and a balance of erosion and deposition at the bottom.

There are two approaches that are commonly used to model the current and sediment profiles and the vertically integrated sediment flux. The first is analytic theory which produces explicit formulas, while the second is the set of turbulence closure models which are usually solved numerically. The analytic approach has the advantage that its results are readily inter-

preted and computationally efficient, but the turbulence closure approach uses a more realistic treatment of the turbulence processes.

One purpose of this memorandum is to show that it is possible to have the advantages of both approaches for at least one turbulence closure model, namely the level 2 model (Mellor and Yamada, 1974, 1982; Lavelle and Mofjeld, 1987a,b) which assumes a local balance at each level in the water column between turbulence production and dissipation. A second purpose is to derive explicit sediment flux formulas for sediment transport studies using the standard log profile for velocity and the Rouse profile for suspended sediment (Rouse, 1937, 1961; Vanoni, 1946; Sleath, 1984) which are relatively good approximations to the profiles from the level 2 model; these formulas are then used to describe the dependence of the suspended sediment flux on the settling velocity, bottom stress, bottom roughness and water depth. The system is assumed to be horizontally homogeneous so that the dynamic quantities vary only with height above the bottom.

The model uses a parabolic form for the mixing length scaled by the depth. As shown by Mofjeld (1988) mixing length limits the application to shallow water in which the depth is small compared to the similarity scale  $u_* / f$ , where  $u_*$  is the friction velocity (square root of the kinematic bottom stress) and  $f$  is the Coriolis parameter. An additional assumption that the currents are uni-directional and parallel with the bottom stress also requires shallow (Mofjeld, 1988) or channelized conditions. The focus is on currents that are driven by barotropic pressure gradients and are the primary source of the turbulence. Hence, effects of wind stress and tidal currents are neglected as are baroclinic pressure gradients. The vertical exchange of momentum and suspended sediment is assumed to be uninhibited by stratification; this limits the application to water that is unstratified by temperature and salinity and to dilute sediment concentrations. Effects of sediment stratification on the bottom boundary layer are discussed, for example, by Adams and Weatherly (1981).

As a bottom boundary condition on the suspended sediment we shall follow Lavelle, Mofjeld and Baker (1984) and Lavelle and Mofjeld (1987a,b) by using a balance between the erosion rate for each settling constituent and its downward settling flux at the bottom rather than the more commonly used reference concentration at a height above the bottom (Sleath, 1984; Vanoni, 1984; van Rijn, 1984). The reasons are that the erosion rate condition is more directly related to physical processes. It also leads to a convenient non-dimensional form for the suspended sediment flux that is the ratio of the horizontal flux per unit area averaged over the water column to the erosion rate which is the upward diffusive flux per area at the bottom.

The theoretical study described in this memorandum makes extensive use of the classic log velocity and Rouse concentration formulas, which as Vanoni (1984) points out occupy a central position in sediment transport theory. A detailed comparison of the log velocity profile and associated eddy viscosity with laboratory observations is given by Nezu and Rodi (1986), and

summary of comparisons between the Rouse concentration profiles with laboratory and field observations is given by van Rijn (1984). Comparisons are given in this memorandum between profiles from various turbulence closure models.

In the sections that follow, a sequence of derivations are given with interpretation. The first section considers the stress profile and shows that it is linear for barotropic pressure-driven currents. The second finds the corresponding eddy viscosity derived from the level 2 turbulence closure model and the parabolic mixing length. The next sections derive in turn the level 2 velocity and suspended sediment formulas and show the close similarity between these and the log velocity and modified Rouse concentration profiles. These sections are followed by a derivation and interpretation of an explicit formula for the vertically integrated suspended sediment flux based on the log and unmodified Rouse profiles.

## 2. STRESS

When steady, uni-directional flow is driven in shallow water by a horizontally uniform, barotropic pressure gradient, the momentum balance is between the pressure gradient and the stress divergence

$$0 = -g \frac{\partial \eta}{\partial x} + \frac{\partial \tau_x}{\partial z} \quad (1)$$

where the pressure gradient is the negative of the surface slope times the acceleration of gravity and  $\tau_x$ , the kinematic stress, is the dynamic stress divided by the constant density. Coriolis effects and channel curvature are neglected.

Integrating (1) upward from the bottom  $z = z_o$  gives a linear profile (Fig. 1) for the stress

$$\tau_x = u_*^2 \left[ \frac{1-z/H}{1-z_o/H} \right] \quad (2)$$

where the stress at the surface  $z = H$  is zero by assumption and the friction velocity  $u_*$  is given by

$$u_* = \left[ -g(H-z_o) \frac{\partial \eta}{\partial x} \right]^{1/2} \quad (3)$$

The linear profile of stress (2) is independent of particular forms assumed for the eddy viscosity and the mixing length and has been verified through observations (e.g., Nezu and Rodi, 1986).

## 3. EDDY VISCOSITY

The level 2 model (Mellor and Yamada, 1974, 1982) takes a very simple form for the turbulence kinetic energy equation in which there is a balance between shear production and dissipation

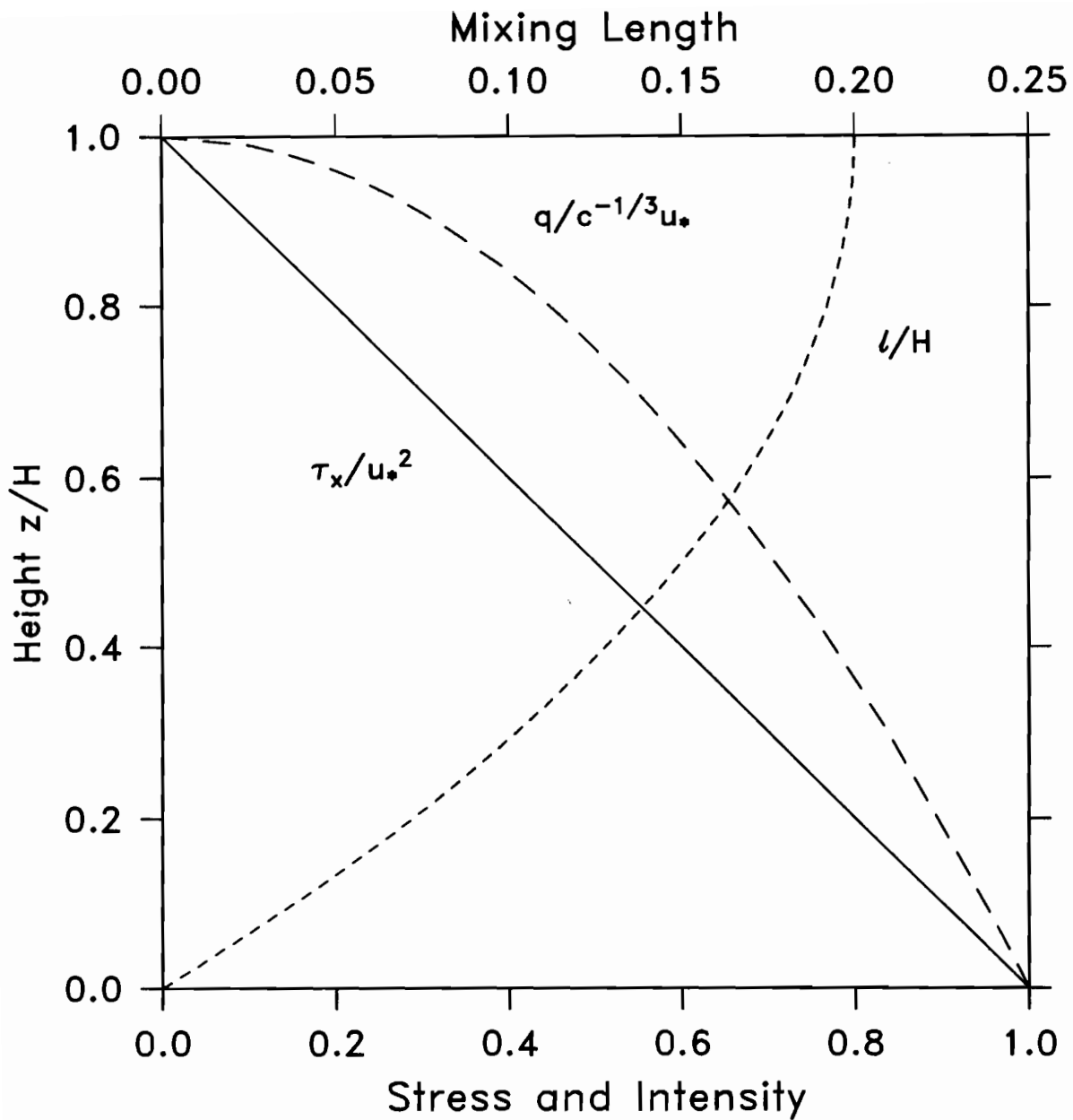


Figure 1. Profiles of stress (Eq. 2; solid line), turbulence intensity (Eq. 8; dashed line) and parabolic mixing length (Eq. 5; dot-dashed line) for steady, unstratified flow in shallow water driven by a horizontally uniform, barotropic pressure gradient.



$$A \left[ \frac{\partial U}{\partial z} \right]^2 - \frac{q^3}{c\ell} = 0 \quad (4)$$

with eddy viscosity  $A$ , velocity  $U$ , height  $z$ , turbulence intensity  $q$  (square root of twice the turbulence kinetic energy divided by the density), empirical dissipation constant  $c$  and mixing length  $\ell$ .

We shall assume that the mixing length  $\ell$  takes a parabolic form (Fig. 2; modified slightly from Lavelle and Mofjeld, 1986)

$$\ell = \kappa z \left[ \frac{1-z/2H}{1-z_0/H} \right] \quad (5)$$

This mixing length is nearly linear  $\ell = \kappa z$  close to the bottom  $z = z_0$  with a vertical gradient equal to von Kármán's constant  $\kappa$ . It is also relatively constant  $\ell = \kappa H / (1 - z_0/H) / 2$  near the surface  $z = H$ .\* The eddy viscosity  $A$  is given by the product of  $q$  and  $\ell$  times a constant equal to  $c^{-1/3}$  (e.g., Mofjeld and Lavelle, 1984)

$$A = c^{-1/3} q \ell \quad (6)$$

Since the kinematic stress  $\tau_x$  is the product of the eddy viscosity and the shear,

$$\tau_x = A \frac{\partial U}{\partial z} \quad (7)$$

the shear can be eliminated from the turbulence kinetic energy equation (4) using (6) and (7) to give a relation between the turbulence intensity  $q$  and the stress  $\tau_x$

$$q = c^{1/3} \tau_x^{1/2} \quad (8)$$

Hence, from (6) and (8) the eddy viscosity can be written as the product of the mixing length  $\ell$  and the square root of the stress

$$A = \ell \tau_x^{1/2} \quad (9)$$

Note that  $A$  in (9) is independent of the dissipation constant  $c$ .

---

\* For deep water, a number of authors (Weatherly and Martin, 1978; Mellor and Yamada, 1982; Du Vachat and Musson-Genon, 1982; Richards, 1982; Mofjeld and Lavelle, 1984; Mofjeld, 1988) have used the Blackadar (1962) form for the mixing length  $\ell$  which approaches an asymptotic value at large heights.

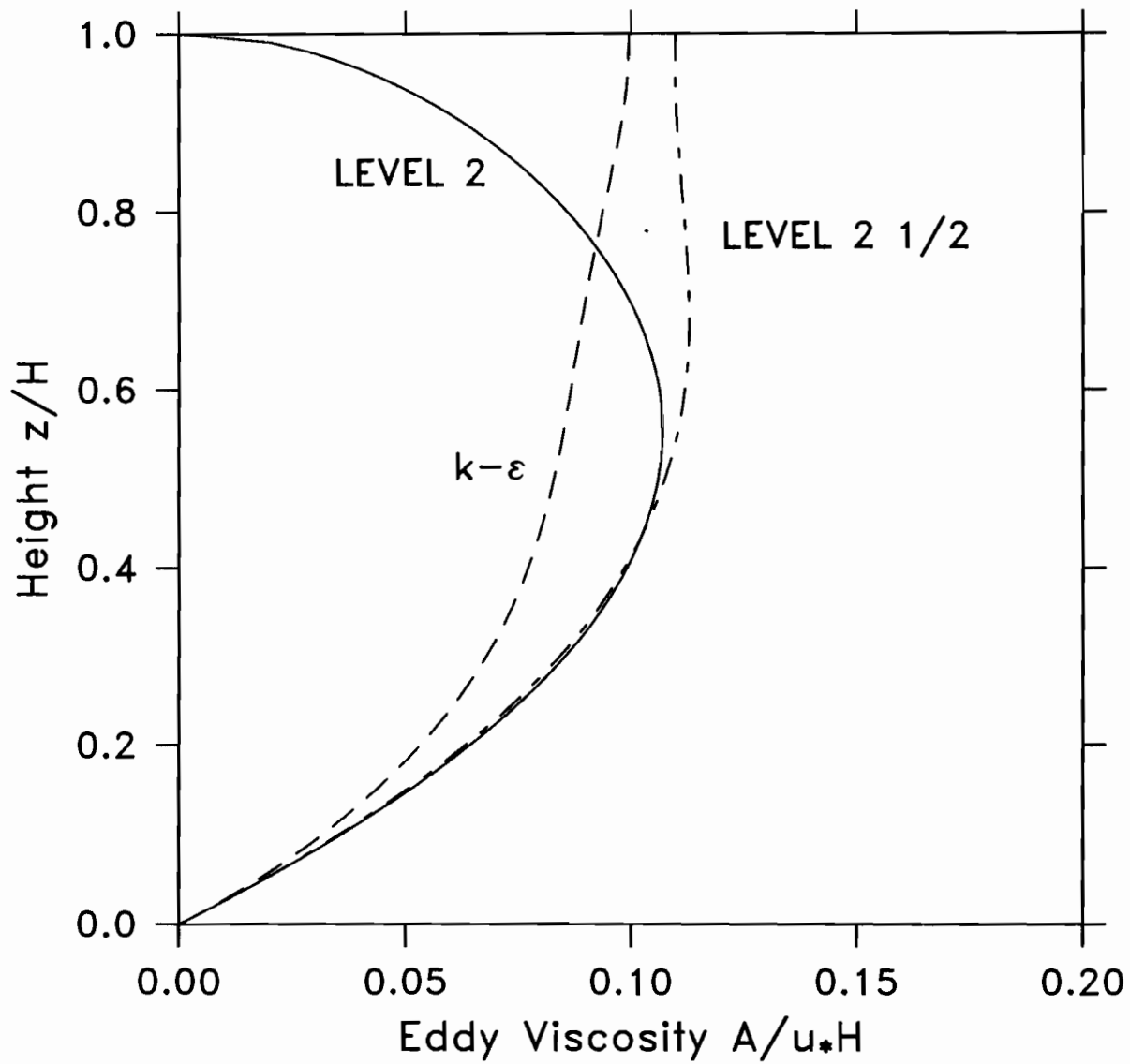


Figure 2. Profiles of the eddy viscosity from the level 2 model (Eq. 10; solid line) for a parabolic mixing length (Eq. 5; dotted line). Also shown are eddy viscosities from a level  $2\frac{1}{2}$  (dot-dashed line) and k- $\epsilon$  (dotted line) model.

The linear forms for the stress (2) and the mixing length (5) lead to an explicit form for the eddy viscosity as a function of height

$$A = \kappa u_* z \frac{(1-z/2H)}{(1-z_0/H)^{3/2}} (1-z/H)^{1/2} \quad (10)$$

Near the bottom  $z = z_0$ , this eddy viscosity is equal to the standard linear form

$$A \doteq \kappa u_* z \quad (11)$$

Shown in Fig. 2 are profiles of eddy viscosity from three models. Near the bottom ( $z \leq .05H$ ) they all have the linear form (11). Higher up the models diverge from the linear profile. The level 2 form (10) is zero at the surface because the surface stress is zero. This shape for the eddy viscosity profile is consistent with the laboratory profiles reported by Nezu and Rodi (1986). The differences in viscosity profiles near the surface do not make a large difference in the profiles of velocity and suspended sediment concentration.

The level  $2\frac{1}{2}$  model (Mellor and Yamada, 1974, 1982; Mofjeld, 1988) gives a slightly smaller eddy viscosity (Fig. 2) than (10) up to  $z \sim 0.7H$  above which it tends to a constant value. The level  $2\frac{1}{2}$  model also uses the prescribed form (5) for the mixing length but differs from the level 2 model in that the turbulence energy equation includes the diffusion of turbulence with a boundary condition that there is no diffusion of turbulence through the surface. Diffusion upward from the large shear zones maintains the turbulent intensity, and hence the eddy viscosity (Fig. 2), at non-zero values near the surface. The k- $\epsilon$  model (Rodi, 1980) does not have a prescribed form for the mixing length. Instead it uses a pair of equations with diffusion to determine the eddy viscosity, one equation being the kinetic energy  $k$  equation while the second is an equation in the dissipation density  $\epsilon$ . The k- $\epsilon$  model gives the smallest eddy viscosity (Fig. 2) up to  $z \sim 0.7H$  and is slightly larger than that of the level  $2\frac{1}{2}$  model very near the surface. The level  $2\frac{1}{2}$  eddy diffusivity can be made to have profiles returning to zero values at the surface (Nezer and Rodi, 1980) by changing the form of the length scale (Eq. 5), as can the k- $\epsilon$  model diffusivity by appropriate choice of surface boundary conditions.

#### 4. VELOCITY

A formula for the velocity  $U$  in terms of the mixing length and stress can be obtained by first solving (7) for the shear and then integrating upward from the bottom  $z = z_0$  to the height  $z$

$$U = \int_{z_0}^z \frac{\tau_x}{A} dz \quad (12)$$

where a no-slip condition  $U = 0$  is assumed at  $z = z_0$ . Using the relation (9) for the eddy viscos-

ity gives the velocity as

$$U = \int_{z_0}^z \frac{\tau_x^{1/2}}{\ell} dz \quad (13)$$

Using the linear stress (2) and mixing length (5) in (12) gives the velocity profile for the level 2 model of steady channel flow

$$U = \frac{u_* \lambda_0}{\kappa} \{ \ln(z/z_0) - 2 \ln[(1+\lambda)/(1+\lambda_0)] + 2[\arctan(\lambda) - \arctan(\lambda_0)] \} \quad (14)$$

where  $\lambda \equiv (1-z/H)^{1/2}$  and  $\lambda_0 \equiv (1-z_0/H)^{1/2}$  (15)

The formula (14) can be put in the form derived by Gross (1984) with different notation. The first term inside the brackets of (14) is the usual logarithmic function of the  $z/z_0$  ratio. The second term ranges from zero at the bottom ( $z = z_0$  and  $\lambda = \lambda_0$ ) to  $-2 \ln(1/2) = 1.39$  at the surface ( $z = H$  and  $Z = 0$ ) when  $z_0 \ll H$ . The third term ranges from  $\doteq \frac{\pi}{2}$  near the bottom to zero at the surface, while the fourth term is a constant near  $\frac{\pi}{2}$ . Hence, the correction terms to the  $\ln(z/z_0)$  term are all order (1) or less and tend to cancel.

The velocity (14) near the bottom takes the standard log form (Schlichting, 1979) expected when the eddy viscosity is the linear form (11) when  $z_0 \ll H$

$$U \doteq \frac{u_*}{\kappa} \ln(z/z_0) \quad (16)$$

A comparison (Fig. 3 and Table 1) shows that the level 2 (14) and the log (16) formulas for velocity give very similar profiles over the entire water column. Near the bottom, they are essentially the same because they are subject to the same eddy viscosity and stress and the same no-slip condition at the bottom. The surface condition of zero stress makes the velocity profile near the surface insensitive to the value of the eddy viscosity.

At the surface, the level 2 velocity (14) is less than the log velocity (16) by a small amount  $[\ln(4) - \pi/2] u_*/\kappa = 0.46 u_*$ . The level  $2\frac{1}{2}$  model produces larger velocities (Fig. 3) than the level 2 model because it includes the upward diffusion of turbulence. This produces a smaller turbulence intensity in the lower part of the water column and hence a smaller eddy viscosity (Fig. 2). To have the same stress (2) the shear must be greater, and this leads to the larger level  $2\frac{1}{2}$  velocity. The k- $\epsilon$  velocity is larger for similar reasons. The level 2 profile can be brought into agreement with the level  $2\frac{1}{2}$  and k- $\epsilon$  model in the upper part of the water column by increasing the value of  $z_0$  by about 50%. The level 2 analysis can be thought of as a justification for the use of the log velocity profile over the full water column for the particular case of steady, uni-directional flow of unstratified water driven by a barotropic pressure gradient. It is not essential

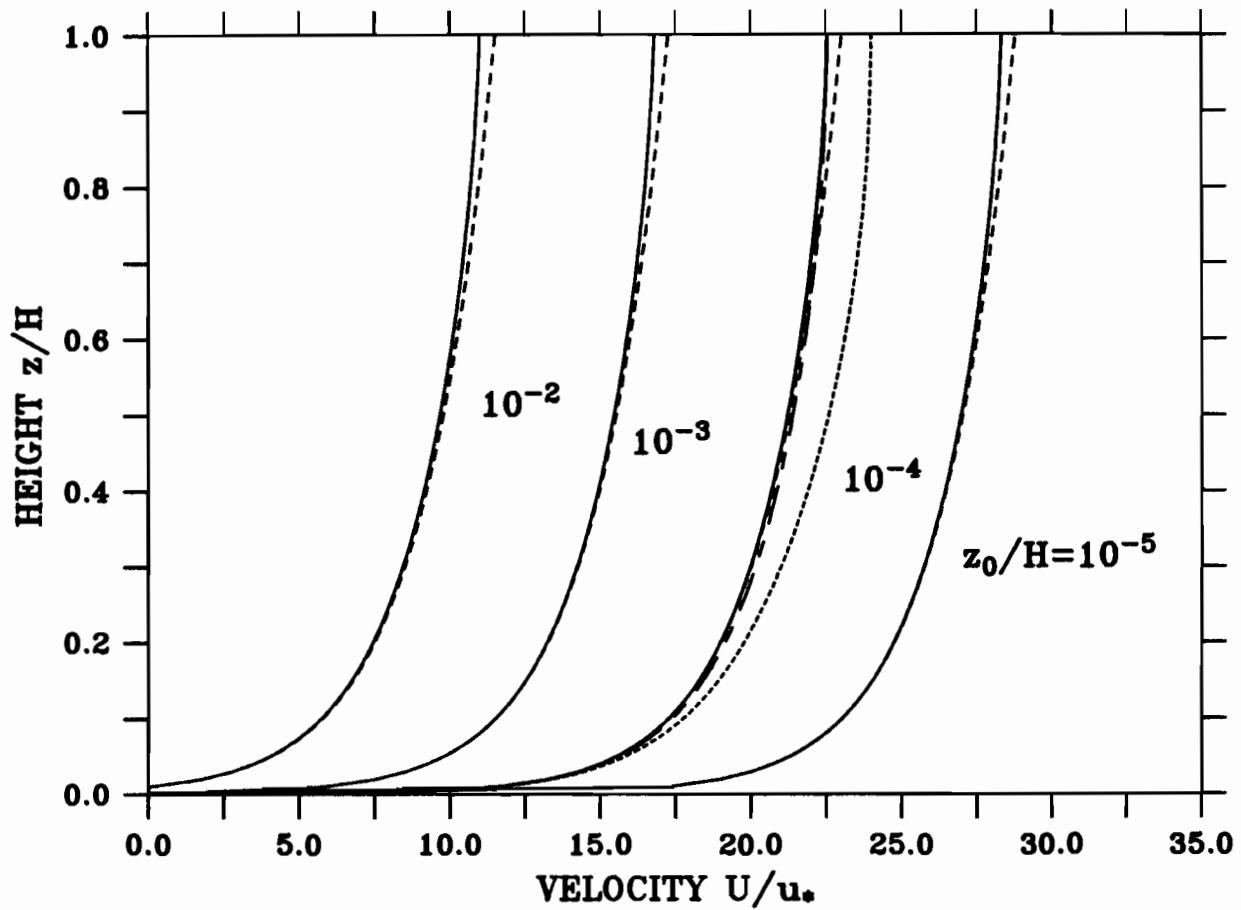


Figure 3. Profiles of velocity from the level 2 model (Eq. 14; solid lines ) and from the log formula (Eq. 16; dashed lines) for different values of the bottom roughness/depth ratio  $z_0/H$ . Also shown are profiles of velocity for  $z_0 = 10^{-4}H$  from a level  $2\frac{1}{2}$  (dot-dashed line) and a k- $\epsilon$  (dotted line) model.

TABLE 1. Velocities at selected heights from the level 2 U (14) and the log U' (16) formulas where the velocities are normalized by the friction velocity  $u_*$ . A positive percentage difference indicates that the log velocity is larger at that height.

$z_o/H = 1.0(10)^{-2}$			
$z/H$	$U/u_*$	$U'/u_*$	% Diff
0.8	10.69	10.96	2.44
0.5	9.67	9.78	1.10
0.2	7.44	7.49	0.60
$z_o/H = 1.0(10)^{-4}$			
$z/H$	$U/u_*$	$U'/u_*$	% Diff
0.8	22.26	22.47	0.93
0.5	21.23	21.29	0.28
0.2	18.99	19.00	0.04
$z_o/H = 1.0(10)^{-6}$			
$z/H$	$U/u_*$	$U'/u_*$	% Diff
0.8	33.77	33.98	0.61
0.5	32.75	32.81	0.18
0.2	30.51	30.52	0.02

that the stress be constant with height and the eddy viscosity increase linearly with height to have a near-log velocity profile.

## 5. SUSPENDED SEDIMENT

The total sediment concentration is assumed to be the sum of concentrations of non-interacting sediment constituents. For a given constituent with settling velocity  $w_s$ , its steady concentration profile  $C(z)$  is determined by a balance between upward diffusion and downward settling

$$A \frac{\partial C}{\partial z} + w_s C = 0 \quad (17)$$

where the subscript for the sediment constituent is deleted. It is assumed in (17) that the eddy diffusivity is equal to the eddy viscosity (Prandtl-Schmidt number equal to one) under the assumptions that the flow is highly turbulent and the suspended sediment is too dilute to stratify the water.

Integrating (18) upward from  $z = z_0$  gives the concentration

$$C = \frac{E}{w_s} \exp \left[ - \int_{z_0}^z \frac{w_s}{A} dz \right] \quad (18)$$

where the boundary condition at the bottom  $z = z_0$  is that the erosion rate  $E$  is equal to the settling flux  $w_s C$  onto the bottom for a steady state. Lavelle and Mofjeld (1984, 1986) show that the erosion rate  $E$  is a strong, power law function of the bottom stress by fitting models to field and laboratory observations.

Using the formula (9) for the eddy viscosity gives a form for the sediment concentration profile as a function of stress  $\tau_x$  and mixing length  $\ell$

$$C = \frac{E}{w_s} \exp \left[ - \int_{z_0}^z \frac{w_s}{\ell \tau_x^{1/2}} dz \right] \quad (19)$$

For the linear stress (2) and mixing length (5) profiles, the suspended sediment concentration takes a power law form

$$C = \frac{E}{w_s} \left[ \frac{z}{z_0} \right]^{-\beta'} \Phi(\lambda) \quad (20)$$

where  $\beta' \equiv w_s \lambda_0^3 / \kappa u_*$  (21)

and  $\Phi(\lambda) \equiv [(1+\lambda)/(1+\lambda_0)]^{2\beta'} \cdot \exp\{2\beta'[\arctan(\lambda) - \arctan(\lambda_0)]\}$  (22)

Near the bottom where  $z \ll H$ , the concentration (20) takes the classic power law

$$C \doteq \frac{E}{w_s} \left( \frac{z}{z_0} \right)^{-\beta} \text{ where } \beta = w_s / \kappa u_* \quad (23)$$

It is useful to compare the level 2 formula (20) over the entire water column with a modified version of the Rouse (1937, 1961) formula for the concentration of suspended sediment

$$C = \frac{E}{w_s} \left[ \frac{z}{z_0} \frac{(H' - z_0)}{(H' - z)} \right]^{-w_s / \kappa u_*} \quad (24)$$

where  $H'$  is a modified depth slightly larger than the actual depth  $H$ . Equation (24) reduces to the original Rouse formula when  $H' = H$ . While Hunt (1954) objects to the Rouse formula as being inconsistent with a linear stress profile, we have seen that these profiles are in fact consistent with the level 2 model (Fig. 3 and Table 1) to a good approximation.

There is good agreement (Fig. 4 and Table 2) between the level 2 and Rouse ( $H' = H$ ) profiles of suspended sediment, except near the surface where the Rouse profile decreases

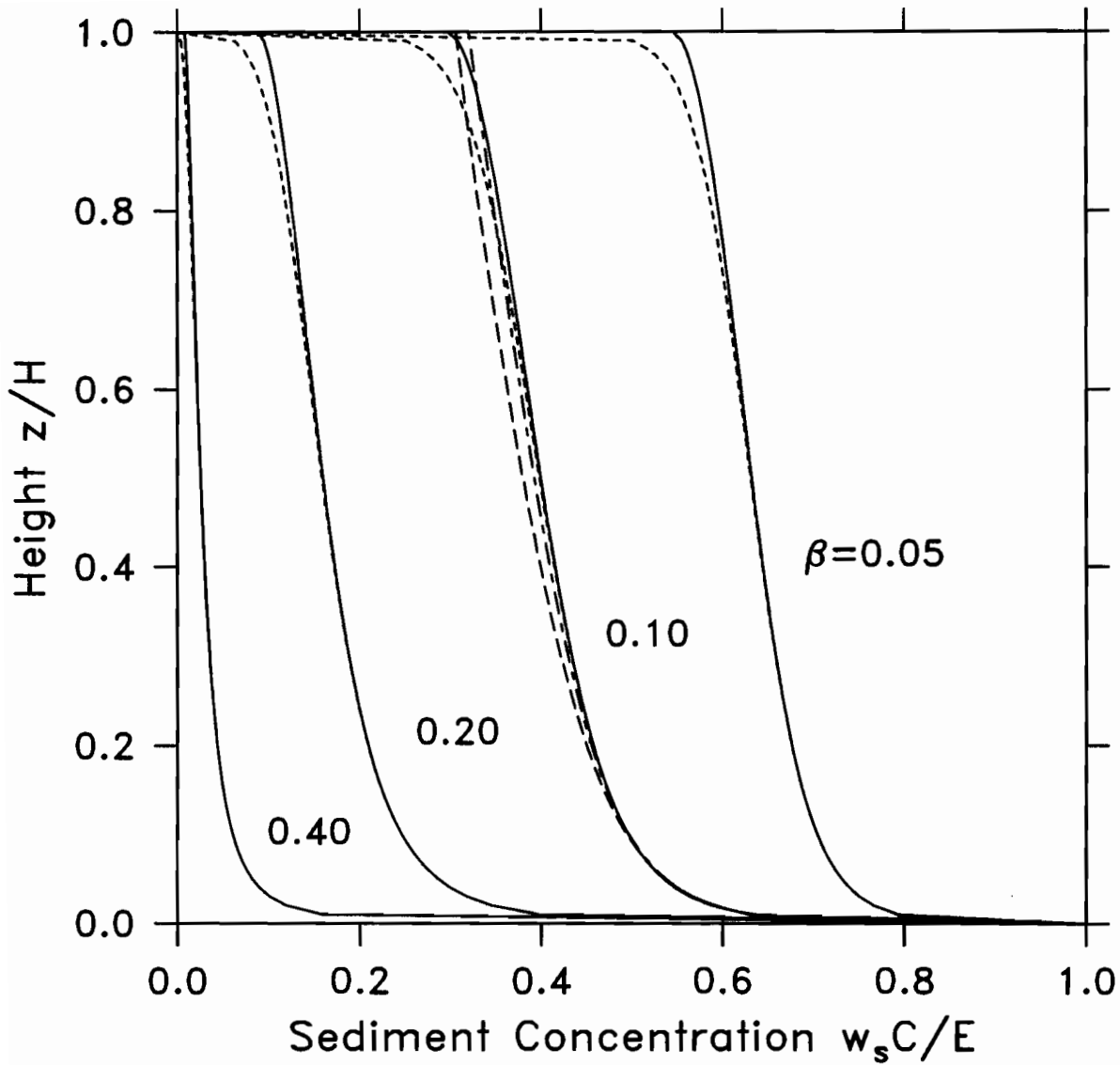


Figure 4. Profiles of suspended sediment concentration from the level 2 model (Eq. 22; solid lines) and from the Rouse formula (Eq. 24; dashed lines) for  $z_0 = 10^{-4}H$  for different values of the settling velocity/friction velocity ratio  $w_s/u_{*}$ . Also shown are profiles of concentration for  $\beta = 0.10$  from a level  $2\frac{1}{2}$  (dot-dashed line) and a k- $\epsilon$  (dotted line) model.



TABLE 2. Suspended sediment concentrations at selected heights from the level 2 C (20) and Rouse C' (24;  $H' = 1.00 H$ ) formulas where the concentrations are normalized by the concentration  $E/w_s$  at the bottom  $z = z_o$ . A negative percentage difference indicates that the Rouse concentration is smaller at that height.

Modified Depth  $H' = 1.00$

$\beta = 0.05$

$z/H$	$z_o/H = 1.0(10)^{-2}$			$z_o/H = 1.0(10)^{-4}$			$z_o/H = 1.0(10)^{-6}$		
	$w_s C/E$	$w_s C'/E$	%Diff	$w_s C/E$	$w_s C'/E$	%Diff	$w_s C/E$	$w_s C'/E$	%Diff
0.8	0.753	0.742	-1.58	0.596	0.589	-1.16	0.473	0.468	-1.16
0.5	0.799	0.795	-0.52	0.632	0.631	-0.19	0.502	0.501	-0.18
0.2	0.854	0.852	-0.26	0.676	0.676	-0.02	0.537	0.537	-0.02

$\beta = 0.10$

$z/H$	$z_o/H = 1.0(10)^{-2}$			$z_o/H = 1.0(10)^{-4}$			$z_o/H = 1.0(10)^{-6}$		
	$w_s C/E$	$w_s C'/E$	%Diff	$w_s C/E$	$w_s C'/E$	%Diff	$w_s C/E$	$w_s C'/E$	%Diff
0.8	0.568	0.550	-3.14	0.355	0.347	-2.32	0.224	0.219	-2.30
0.5	0.638	0.632	-1.04	0.400	0.398	-0.38	0.252	0.251	-0.37
0.2	0.729	0.726	-0.51	0.458	0.457	-0.05	0.289	0.289	-0.03

$\beta = 0.20$

$z/H$	$z_o/H = 1.0(10)^{-2}$			$z_o/H = 1.0(10)^{-4}$			$z_o/H = 1.0(10)^{-6}$		
	$w_s C/E$	$w_s C'/E$	%Diff	$w_s C/E$	$w_s C'/E$	%Diff	$w_s C/E$	$w_s C'/E$	%Diff
0.8	0.322	0.302	-6.18	0.126	0.120	-4.58	0.050	0.048	-4.55
0.5	0.407	0.399	-2.07	0.160	0.158	-0.76	0.064	0.063	-0.73
0.2	0.532	0.526	-1.02	0.209	0.209	-0.09	0.083	0.083	-0.07

$\beta = 0.40$

$z/H$	$z_o/H = 1.0(10)^{-2}$			$z_o/H = 1.0(10)^{-4}$			$z_o/H = 1.0(10)^{-6}$		
	$w_s C/E$	$w_s C'/E$	%Diff	$w_s C/E$	$w_s C'/E$	%Diff	$w_s C/E$	$w_s C'/E$	%Diff
0.8	0.104	0.091	-11.97	0.016	0.014	-8.94	0.003	0.002	-8.89
0.5	0.166	0.159	-4.11	0.026	0.025	-1.51	0.004	0.004	-1.45
0.2	0.283	0.277	-2.03	0.044	0.044	-0.18	0.007	0.007	-0.13

unrealistically to zero concentration. All the theoretical profiles (Fig. 4) match the power law (23) near the bottom. Setting  $H' = 1.07 H$  brings the modified Rouse profile (Fig. 5 and Table 3) into close agreement with the level 2 and other closure models.

## 6. SUSPENDED SEDIMENT FLUX

For steady conditions, the suspended sediment flux per unit width (sediment flux hereafter) is the integral over the water column of the velocity times the sediment concentration

$$F = \int_{z_0}^H U C dz \quad (25)$$

It is convenient to normalize the sediment flux  $F$  (25) by the product of the erosion rate  $E$  for the settling constituent and the depth  $H$ . The ratio  $F/EH$  can be thought of as the ratio of the average horizontal flux  $F/H$  per unit area to the upward diffusive flux  $E$  per unit area at the bottom. The non-dimensionalized sediment flux  $F/EH$  is then a function of the two ratios  $z_0/H$  and  $\beta = w_s/\kappa u_*$ .

As seen in Table 4, the non-dimensionalized sediment flux is a sensitive function of  $\beta$ , decreasing over many orders of magnitude with increasing  $\beta$ . The comparison in Table 4 shows that the value of the sediment flux is relatively insensitive to the forms of the velocity and sediment concentration profiles. For  $z_0/H \leq 1.0(10)^{-3}$ , the best fit (within 1%) of the sediment flux derived from the log velocity (16) and modified Rouse concentration (24) profiles to the sediment flux from the level 2 velocity (14) and concentration (20) occurs for a modified depth  $H' = 1.05 H$ , slightly less than the best fit modified depth  $H' = 1.07 H$  for the sediment concentration (Table 3 and Fig. 5). However, the unmodified Rouse profile yields a flux that is within 3% of the level 2 value for  $z_0/H \leq 1.0(10)^{-3}$ .

The log velocity and unmodified Rouse concentration profiles have the advantage that they lead directly to a set of explicit formulas for the sediment flux that can be interpreted readily. For these profiles, the sediment flux has the form

$$F = \frac{E H}{\kappa^2 \beta} \left[ \frac{Z_0}{1-Z_0} \right]^\beta \int_{z_0}^1 \ln(Z/Z_0) Z^\beta (1-Z)^\beta dz \quad (26)$$

where  $Z = z/H$ ,  $Z_0 = z_0/H$  and  $\beta = w_s/\kappa u_*$ .

### A. Slow Settling Velocity (or High Bed Stress) $\beta < 1$

When  $\beta$  is less than one, the integral in (26) can be put into standard form as the difference of two improper integrals – one from 0 to 1 and a correction from 0 to  $Z_0$  in which  $(1-z)^\beta$  is set to one. After putting these integrals into standard form (Gradshteyn and Ryzhik, 1980) the flux formula for  $\beta < 1$  is then

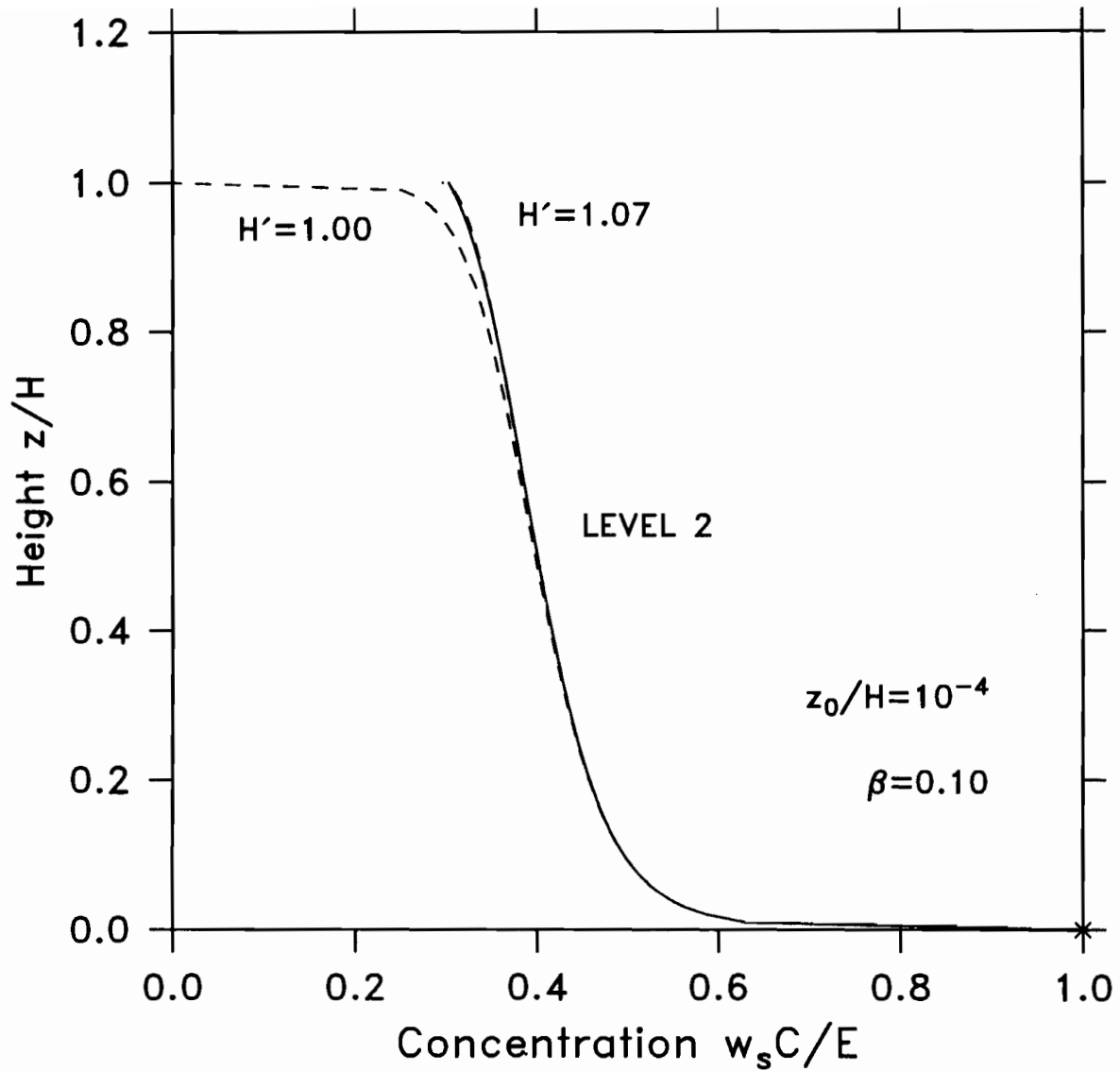


Figure 5. Profiles of suspended sediment concentration from the level 2 model (Eq. 22; solid line) and from the modified Rouse formula (24) for modified depth  $H' = 1.07H$  (dashed line) and  $H' = 1.00H$  (dot-dashed line).

TABLE 3. Suspended sediment concentrations at selected heights from the level 2 C (20) and modified Rouse C' (24;  $H' = 1.07 H$ ) formulas where the concentrations are normalized by the concentration  $E/w_s$  at the bottom  $z = z_0$ . A positive percentage difference indicates that the Rouse concentration is larger at that height.

Modified Depth  $H' = 1.07$

$\beta = 0.05$

$z/H$	$z_0/H = 1.0(10)^{-2}$			$z_0/H = 1.0(10)^{-4}$			$z_0/H = 1.0(10)^{-6}$		
	$w_s C/E$	$w_s C'/E$	%Diff	$w_s C/E$	$w_s C'/E$	%Diff	$w_s C/E$	$w_s C'/E$	%Diff
0.8	0.753	0.750	-0.43	0.596	0.596	-0.01	0.473	0.473	0.00
0.5	0.799	0.797	-0.21	0.632	0.633	0.13	0.502	0.503	0.13
0.2	0.854	0.852	-0.18	0.676	0.677	0.06	0.537	0.538	0.06

$\beta = 0.10$

$z/H$	$z_0/H = 1.0(10)^{-2}$			$z_0/H = 1.0(10)^{-4}$			$z_0/H = 1.0(10)^{-6}$		
	$w_s C/E$	$w_s C'/E$	%Diff	$w_s C/E$	$w_s C'/E$	%Diff	$w_s C/E$	$w_s C'/E$	%Diff
0.8	0.568	0.563	-0.87	0.355	0.355	-0.02	0.224	0.224	0.00
0.5	0.638	0.636	-0.42	0.400	0.401	0.25	0.252	0.253	0.27
0.2	0.729	0.727	-0.36	0.458	0.458	0.12	0.289	0.289	0.13

$\beta = 0.20$

$z/H$	$z_0/H = 1.0(10)^{-2}$			$z_0/H = 1.0(10)^{-4}$			$z_0/H = 1.0(10)^{-6}$		
	$w_s C/E$	$w_s C'/E$	%Diff	$w_s C/E$	$w_s C'/E$	%Diff	$w_s C/E$	$w_s C'/E$	%Diff
0.8	0.322	0.317	-1.72	0.126	0.126	-0.04	0.050	0.050	-0.01
0.5	0.407	0.404	-0.84	0.160	0.161	0.51	0.064	0.064	0.54
0.2	0.532	0.528	-0.71	0.209	0.210	0.23	0.083	0.084	0.26

$\beta = 0.40$

$z/H$	$z_0/H = 1.0(10)^{-2}$			$z_0/H = 1.0(10)^{-4}$			$z_0/H = 1.0(10)^{-6}$		
	$w_s C/E$	$w_s C'/E$	%Diff	$w_s C/E$	$w_s C'/E$	%Diff	$w_s C/E$	$w_s C'/E$	%Diff
0.8	0.104	0.100	-3.42	0.016	0.016	-0.07	0.003	0.003	-0.01
0.5	0.166	0.163	-1.67	0.026	0.026	1.02	0.004	0.004	1.08
0.2	0.283	0.279	-1.42	0.044	0.044	0.47	0.007	0.007	0.52

TABLE 4. Comparison of sediment fluxes per unit width obtained from the level 2 formulas for velocity (14) and sediment concentration (20) with fluxes obtained from the log velocity (16) and modified Rouse concentration (24). The fluxes are computed numerically over a height grid that is stretched at the bottom and the surface. A positive percentage difference indicates that the log-Rouse flux is larger.

For  $z_0/H = 1.0(10)^{-2}$

$\beta$	Level 2	Log-Rouse ( $H' = 1.00 H$ )		Log-Rouse ( $H' = 1.05 H$ )	
	F/EH	F/EH	% Diff	F/EH	% Diff
0.0100	$2.119(10)^3$	$2.149(10)^3$	1.40	$2.153(10)^3$	1.58
0.0316	$6.056(10)^2$	$6.102(10)^2$	0.76	$6.135(10)^2$	1.32
0.1000	$1.397(10)^2$	$1.383(10)^2$	-0.97	$1.404(10)^2$	0.54
0.3162	$1.713(10)^1$	$1.640(10)^1$	-4.28	$1.691(10)^1$	-1.31
1.0000	$4.683(10)^{-1}$	$4.412(10)^{-1}$	-5.79	$4.519(10)^{-1}$	-3.51
3.1623	$4.089(10)^{-3}$	$3.939(10)^{-3}$	-3.68	$3.951(10)^{-3}$	-3.37

For  $z_0/H = 1.0(10)^{-3}$

$\beta$	Level 2	Log-Rouse ( $H' = 1.00 H$ )		Log-Rouse ( $H' = 1.05 H$ )	
	F/EH	F/EH	% Diff	F/EH	% Diff
0.0100	$3.419(10)^3$	$3.437(10)^3$	0.55	$3.443(10)^3$	0.73
0.0316	$9.309(10)^2$	$9.318(10)^2$	0.10	$9.366(10)^2$	0.61
0.1000	$1.846(10)^2$	$1.826(10)^2$	-1.09	$1.851(10)^2$	0.29
0.3162	$1.423(10)^1$	$1.381(10)^1$	-2.95	$1.419(10)^1$	-0.29
1.0000	$1.144(10)^{-1}$	$1.123(10)^{-1}$	-1.85	$1.141(10)^{-1}$	-0.31
3.1623	$4.211(10)^{-4}$	$4.195(10)^{-4}$	-0.39	$4.197(10)^{-4}$	-0.35

For  $z_0/H = 1.0(10)^{-4}$

$\beta$	Level 2	Log-Rouse ( $H' = 1.00 H$ )		Log-Rouse ( $H' = 1.05 H$ )	
	F/EH	F/EH	% Diff	F/EH	% Diff
0.0100	$4.656(10)^3$	$4.671(10)^3$	0.32	$4.679(10)^3$	0.49
0.0316	$1.208(10)^3$	$1.207(10)^3$	-0.10	$1.213(10)^3$	0.40
0.1000	$2.056(10)^2$	$2.032(10)^2$	-1.16	$2.059(10)^2$	0.16
0.3162	$9.844(10)^0$	$9.580(10)^0$	-2.68	$9.827(10)^0$	-0.18
1.0000	$2.160(10)^{-2}$	$2.138(10)^{-2}$	-1.00	$2.162(10)^{-2}$	0.13
3.1623	$4.226(10)^{-5}$	$4.224(10)^{-5}$	-0.05	$4.224(10)^{-5}$	-0.04

For  $z_0/H = 1.0(10)^{-5}$

$\beta$	Level 2	Log-Rouse ( $H' = 1.00 H$ )		Log-Rouse ( $H' = 1.05 H$ )	
	F/EH	F/EH	% Diff	F/EH	% Diff
0.0100	$5.836(10)^3$	$5.848(10)^3$	0.21	$5.857(10)^3$	0.37
0.0316	$1.442(10)^3$	$1.439(10)^3$	-0.19	$1.446(10)^3$	0.29
0.1000	$2.102(10)^2$	$2.077(10)^2$	-1.22	$2.104(10)^2$	0.08
0.3162	$6.201(10)^0$	$6.039(10)^0$	-2.61	$6.189(10)^0$	-0.20
1.0000	$3.511(10)^{-3}$	$3.485(10)^{-3}$	-0.73	$3.516(10)^{-3}$	0.16
3.1623	$4.234(10)^{-6}$	$4.227(10)^{-6}$	-0.16	$4.227(10)^{-6}$	-0.16

$$F = \frac{EH}{\kappa^2 \beta} \left[ \frac{Z_o}{1-Z_o} \right]^\beta \left\{ \frac{\beta\pi}{\sin(\beta\pi)} [-\ln(Z_o) + \psi(1-\beta) - \psi(2)] + Z_o(1-Z_o)^{-\beta} (1-\beta)^{-2} \right\} \quad (27)$$

where the difference in digamma functions is (Abramowitz and Stegun, 1965)

$$\psi(1-\beta) - \psi(2) = -\frac{1}{2\beta} + \frac{\pi}{2} \cot(\beta\pi) - (1-\beta^2)^{-1} - \theta(\beta) \quad (28)$$

with coefficients of the rapidly converging series

$$\theta(\beta) = \sum_{n=1}^{\infty} [\zeta(2n+1) - 1] \beta^{2n} \quad (29)$$

given in Table 5; the factor  $\frac{\beta\pi}{\sin(\beta\pi)}$  is a special form of the complete beta function  $B(1-\beta, 1+\beta)$  for  $\beta < 1$ .

Shown in Fig. 6 are the contributions of the various terms in the flux formula (27) arising from the integral in (26) as functions of  $\beta$  where

$$\begin{aligned} T_0 &= \kappa^{-2} \beta^{-1} \quad , \quad T_1 = Z_o^\beta (1 - Z_o)^{-\beta}, \\ T_2 &= \frac{\beta\pi}{\sin(\beta\pi)} [-\ln(Z_o) + \psi(1-\beta) - \psi(2)], \\ T_3 &= Z_o(1-Z_o)^{-\beta} (1-\beta)^{-2} \quad , \quad F/EH = T_0(T_1 T_2 + T_3) \end{aligned} \quad (30)$$

For  $\beta < 0.1$ , the variations (Fig. 6) of  $F/EH$  with  $\beta$  are due to  $\beta^{-1}$  in  $T_0$  while at larger  $\beta$  the  $Z_o^\beta$  factor in  $T_1$  also contributes significantly. Only near  $\beta = 1$  do the other terms  $T_2$  and  $T_3$  vary greatly in response to the singularities at  $\beta = 1$ .

TABLE 5. Coefficients of the  $\theta(\beta)$  function (27) in the formula (26) for suspended load transport for  $\beta < 1$  where  $\zeta(2n+1)$  is the Riemann zeta function for odd integers (Abramowitz and Stegun, 1965).

n	$\zeta(2n+1) - 1$	n	$\zeta(2n+1) - 1$
1	0.2020569	6	0.0001227
2	0.0369278	7	0.0000306
3	0.0083493	8	0.0000076
4	0.0020084	9	0.0000019
5	0.0004942	10	0.0000005

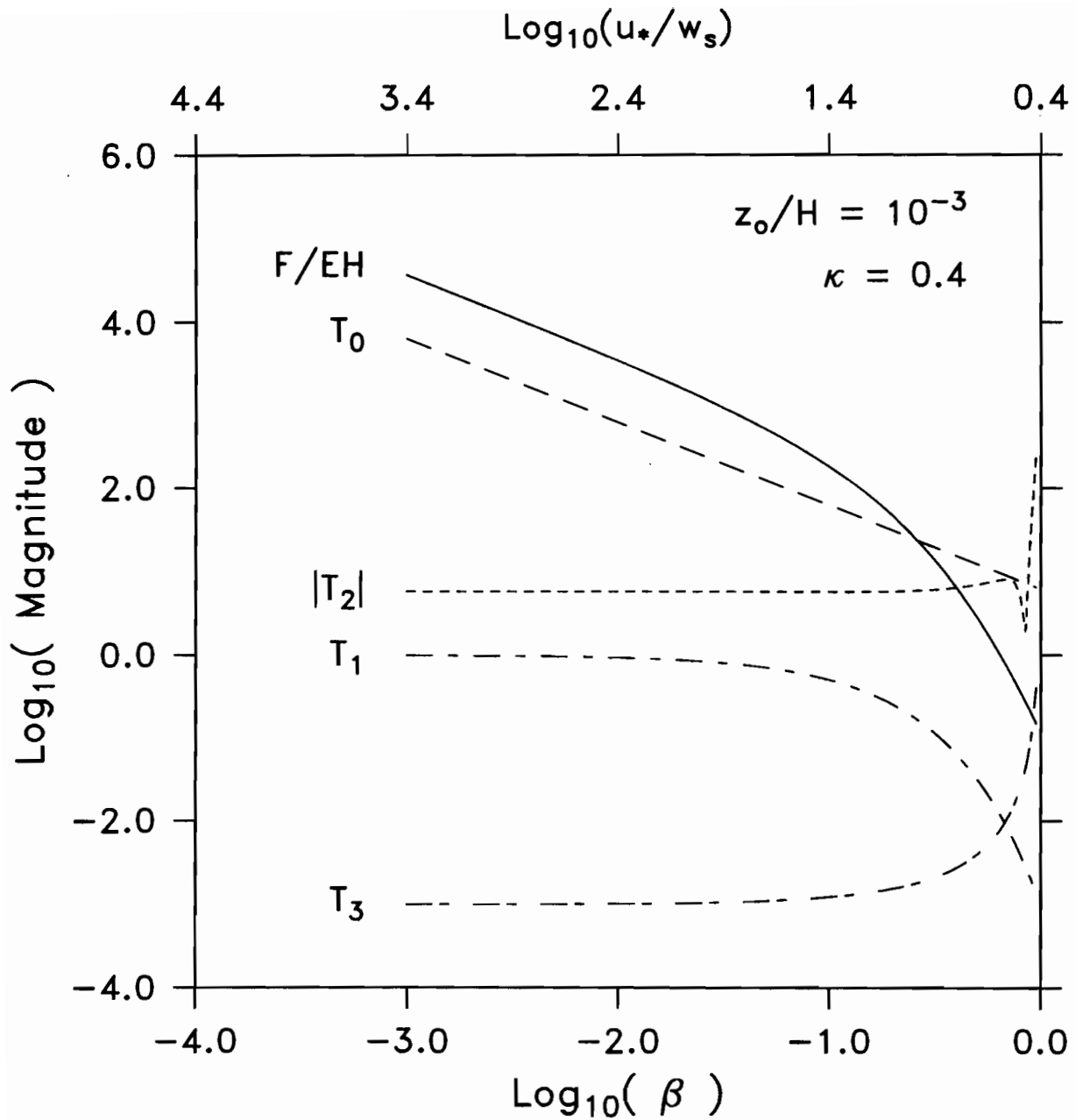


Figure 6. Terms (30) in the formula (27) for the normalized suspended sediment flux  $F/EH$  per unit width as functions of  $\beta = w_s/\kappa u_*$  for  $\beta < 1$ .

An approximate flux formula, accurate within ~4% (Fig. 7), can therefore be used

$$F = \frac{E H}{\kappa^2 \beta} (z_o/H)^\beta \ln(H/ez_o) \quad \text{for } \beta < 0.2 \quad (31)$$

where  $e = 2.71828$  is the base of the natural logarithm. The factor  $\ln(H/ez_o)/\kappa$  is the vertically averaged velocity per unit  $u_*$ , while  $(z_o/H)$  arises from the sediment concentration  $C$  at the bottom  $z = z_o$ ; both  $U$  and  $C$  contribute to the factor  $\kappa^{-1}\beta^{-1}$ .

While the full flux formula (27) is indeterminate at  $\beta = 1$ , it converges (Fig. 6) toward the special expression

$$F = \frac{E H}{\kappa^2 \beta} \left[ \frac{1}{2} \ln^2(H/z_o) - \ln(H/z_o) + 1 - z_o/H \right] \text{ at } \beta = 1 \quad (32)$$

### B. Fast Settling Velocity (or Low Bed Stress) $\beta \geq 2$

For settling velocities  $w_s$  comparable with or greater than the friction velocity  $u_*$ , the bulk of the suspended sediment lies near the bottom. It is reasonable therefore that an asymptotic formula for very large depth should be a good approximation

$$F = \frac{E H}{\kappa^2 \beta} \frac{1}{(\beta-1)^2} \left( \frac{z_o}{H} \right) \quad \text{for } \beta \geq 2 \quad (33)$$

as is found to be the case for integer  $\beta \geq 2$  (Table 6). Only in the relatively extreme cases (Table 6) of  $z_o/H = 10^{-2}$  and  $\beta = 2.0$ ,  $z_o/H = 10^{-3}$  does the flux from (33) differ by more than 1% from the numerically computed flux.

### C. Transitional Settling Velocity $1 \leq \beta < 2$

While a complete formula analogous to (27) can be found for the gap in the sediment flux formulas between the fast and slow settling regimes, it is more convenient to interpolate over this relatively small domain in  $\beta$  between flux values at  $\beta_1 = 2.0$  and  $\beta_2 = 0.95$ . This domain also spans over the indefinite value of (27) at  $\beta = 1$ . Since the flux formulas (27) and (33) involve products of terms that are often raised to powers, it is appropriate to logarithmically interpolate the sediment flux  $F$ . This is equivalent to the formula

$$F = F_1 (\beta/\beta_1)^r \quad \text{with } r = \frac{\log(F_2/F_1)}{\log(\beta_2/\beta_1)} \quad \text{for } 0.95 < \beta < 2 \quad (34)$$

where  $F_1$  is the asymptotic formula (33) evaluated at  $\beta_1 = 2$  and  $F_2$  is the formula (27) for  $\beta_2 = 0.95$ .



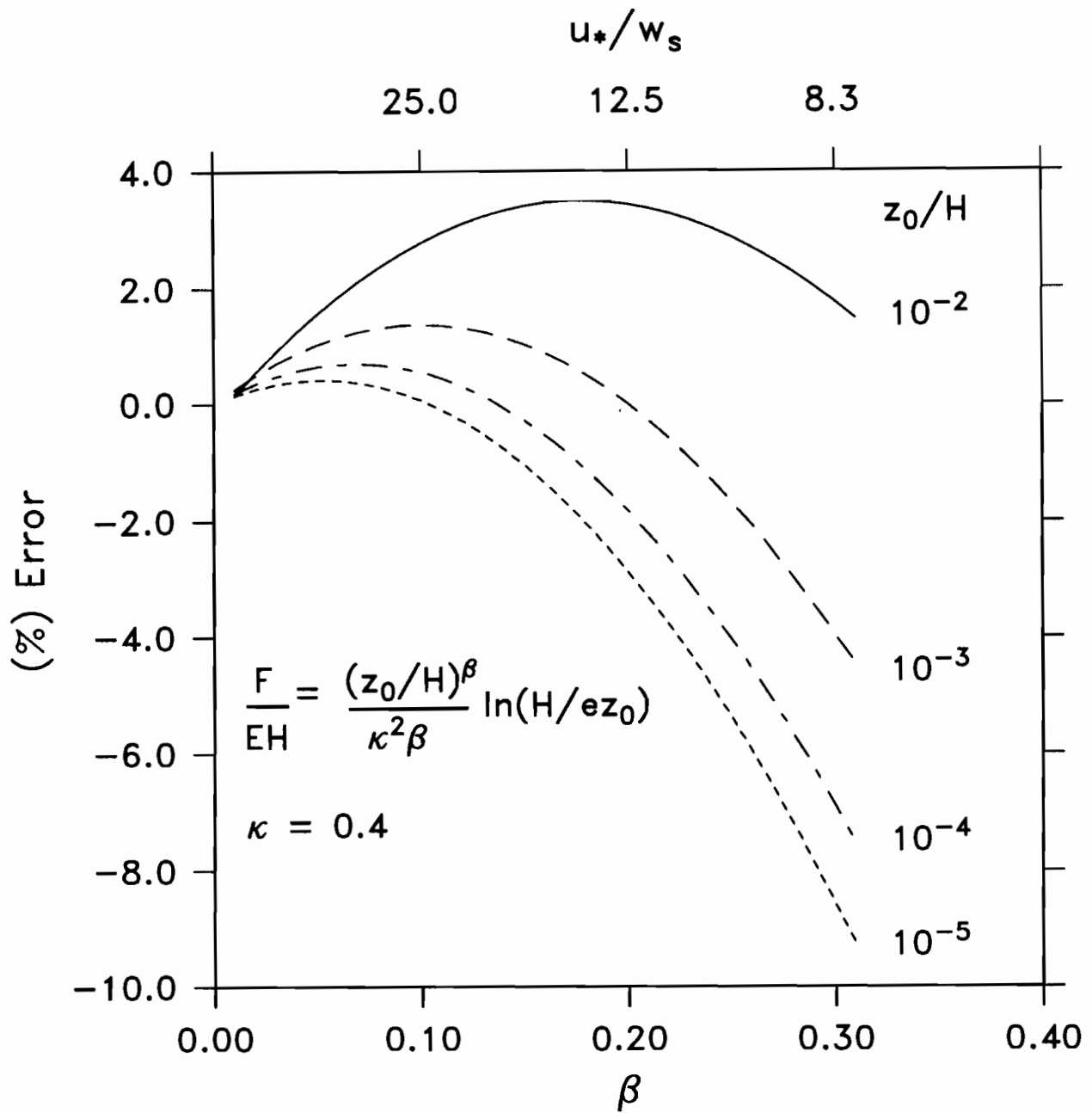


Figure 7. Percentage error between the approximate formula (31) for the normalized suspended sediment flux  $F/EH$  per unit width assuming  $\beta = w_s/Ku_* \ll 1$  and the exact formula (27).

TABLE 6. Comparison of the asymptotic formula (33) for the sediment flux  $F/EH$  at large  $\beta$  with the numerical integration over the water column of the product of the log velocity and unmodified ( $H' = H$ ) Rouse concentration profiles. A positive difference indicates that the asymptotic formula gives a larger transport.

For  $z_0/H = 1.0(10)^{-2}$

$\beta$	Numerical F/EH	Asymptotic F/EH	% Diff
2.0	$2.449(10)^{-2}$	$3.125(10)^{-2}$	27.61
3.0	$4.815(10)^{-3}$	$5.208(10)^{-3}$	8.17
4.0	$1.653(10)^{-3}$	$1.736(10)^{-3}$	5.00
5.0	$7.517(10)^{-4}$	$7.812(10)^{-4}$	3.94
6.0	$4.029(10)^{-4}$	$4.167(10)^{-4}$	3.43

For  $z_0/H = 1.0(10)^{-3}$

$\beta$	Numerical F/EH	Asymptotic F/EH	% Diff
2.0	$2.976(10)^{-3}$	$3.125(10)^{-3}$	5.02
3.0	$5.163(10)^{-4}$	$5.208(10)^{-4}$	0.88
4.0	$1.727(10)^{-4}$	$1.736(10)^{-4}$	0.50
5.0	$7.782(10)^{-5}$	$7.812(10)^{-5}$	0.39
6.0	$4.153(10)^{-5}$	$4.167(10)^{-5}$	0.34

For  $z_0/H = 1.0(10)^{-4}$

$\beta$	Numerical F/EH	Asymptotic F/EH	% Diff
2.0	$3.098(10)^{-4}$	$3.125(10)^{-4}$	0.86
3.0	$5.204(10)^{-5}$	$5.208(10)^{-5}$	0.09
4.0	$1.735(10)^{-5}$	$1.736(10)^{-5}$	0.05
5.0	$7.809(10)^{-6}$	$7.812(10)^{-6}$	0.04
6.0	$4.165(10)^{-6}$	$4.167(10)^{-6}$	0.03

For  $z_0/H = 1.0(10)^{-5}$

$\beta$	Numerical F/EH	Asymptotic F/EH	% Diff
2.0	$3.121(10)^{-5}$	$3.125(10)^{-5}$	0.13
3.0	$5.208(10)^{-6}$	$5.208(10)^{-6}$	0.01
4.0	$1.736(10)^{-6}$	$1.736(10)^{-6}$	0.01
5.0	$7.812(10)^{-7}$	$7.812(10)^{-7}$	0.00
6.0	$4.167(10)^{-7}$	$4.167(10)^{-7}$	0.00

#### D. General Dependence of F/EH on $\beta$ and $z_o/H$

In general the ratio F/EH (Fig. 8) depends more strongly on  $\beta$  than  $z_o/H$ . As discussed earlier the ratio at small  $\beta$  ( $<0.1$ ) varies inversely with  $\beta$ ; it decreases more rapidly at larger  $\beta$  with a  $\beta^{-1}(\beta-1)^{-2}$  dependence for  $\beta \geq 2$ . At small  $\beta$  ( $<0.1$ ) the ratio F/EH decreases slowly with increasing  $z_o/H$  but increases at larger  $\beta$ , becoming proportional to  $z_o/H$  at  $\beta$  greater than  $\sim 2$ . The sediment flux F is therefore proportional (31) to  $H \ln(H/ez_o)$  at small  $\beta$  but essentially independent of depth H for large  $\beta$  for which the suspended sediment resides near the bottom.

The sediment flux F (26) depends on the friction velocity  $u_*$  through  $\beta$  but also through the erosion rate E. The latter dependence can dominate when E is a strong function of  $u_*$  as is seen when E follows the power law in the bottom stress observed by Lavelle, Mofjeld and Baker (1984) and Lavelle and Mofjeld (1987a). This is particularly true when  $\beta$  is small. In practice the differences between the sediment flux formulas derived from the level 2 or log velocity and Rouse concentration profiles or between the degree of approximation in the explicit flux formulas are most likely overwhelmed by the uncertainties in estimates of the settling velocity, bottom stress and coefficients in the erosion law.

## 7. CONCLUSIONS

For a shallow steady pressure-driven flow, the level 2 turbulence closure model leads to analytic formulas for the profiles of stress, eddy viscosity, velocity, turbulence intensity and suspended sediment concentration. The level 2 velocity formula agrees closely with the classic log profile, and the level 2 suspended sediment formula agrees with a modified Rouse formula (depth H replaced by  $1.07H$ ). These results give a theoretical justification for the use of the log velocity and modified Rouse formulas for over the entire water column for shallow steady pressure-driven flow. There is close agreement between the vertically integrated sediment flux from the level 2 and classic log velocity and unmodified Rouse concentration profiles. The latter give rise to a set of explicit formulas for the flux that can be readily interpreted.

## 8. ACKNOWLEDGMENTS

This work was supported by the Environmental Research Laboratory, National Oceanic and Atmospheric Administration, and by the Office of Marine Pollution Assessment under the LRERP/Sec. 202 Program. The authors wish to thank Lisa Lytle for preparing the figures on the PMEL VAX computers.

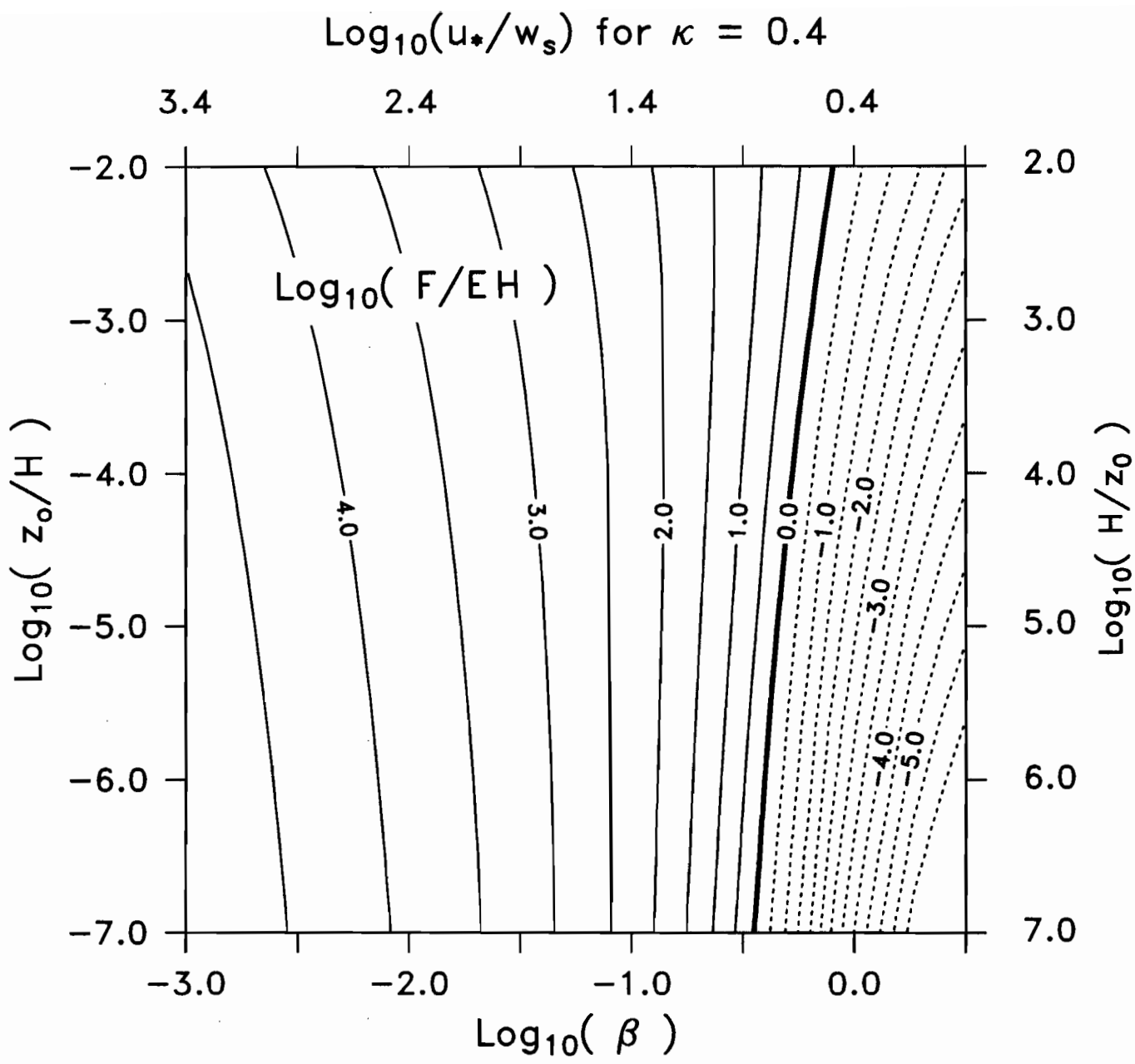


Figure 8. The logarithm of the normalized suspended sediment flux  $F/EH$  per unit width as a function of  $\beta = w_s/Ku_*$  and the ratio  $z_0/H$  obtained from (27) for  $\beta \leq 0.95$ , from (34) for  $0.95 < \beta < 2.0$  and from (33) for  $\beta \geq 2.0$ .

## 9. REFERENCES

- Abramowitz, M., and I.A. Stegun, 1965. *Handbook of Mathematical Functions*. Dover, New York, 1046 pp.
- Adams, C.E., and G.L. Weatherly, 1981. Some effects of suspended sediment stratification on an oceanic boundary layer. *J. Geophys. Res.*, *86*, 4161-4172.
- Blackadar, A.K., 1962. The vertical distribution of wind and turbulent exchange in a neutral atmosphere. *J. Geophys. Res.*, *67*, 3095-3120.
- Du Vachat, R., and L. Musson-Genon, 1982. Rossby similarity and turbulent formulation. *Boundary-Layer Meteorol.*, *23*, 47-68.
- Gradshteyn, I.S., and I.M. Ryzhik, 1980. *Table of Integrals, Series and Products*. Academic Press, New York, 1160 pp.
- Gross, T., 1984. Tidal time dependence of geophysical turbulent boundary layers. PhD. Dissertation, University of Washington, Seattle, 161 pp.
- Hunt, J.N., 1954. The turbulent transport of suspended sediment in open channels. *Proc. R. Soc. London., Ser. A*, *224*, 322-335.
- Lavelle, J.W., and H.O. Mofjeld, 1987a. Do critical stresses for incipient motion and erosion really exist? *J. Hydraulic Eng.*, *113*(3), 370-385.
- Lavelle, J.W., and H.O. Mofjeld, 1987b. Bibliography on sediment threshold velocity. *J. Hydraul. Eng.*, *113*(3), 389-393.
- Lavelle, J.W., H.O. Mofjeld, and E.T. Baker, 1984. An in situ erosion rate for a fine-grained marine sediment. *J. Geophys. Res.*, *89*, 6543-6552.
- Mellor, G.L., and T. Yamada, 1974. A hierarchy of turbulence closure models for planetary boundary layers. *J. Atmos. Sci.*, *31*, 1791-1806. (Corridentium, 1977. *J. Atmos. Sci.*, *34*, 1482)
- Mellor, G.L., and T. Yamada, 1982. Development of a turbulence closure model for geophysical fluid problems. *Rev. Geophys. Space Phys.*, *20*, 851-875.
- Mofjeld, H.O., 1988. The depth dependence of bottom stress and quadratic drag coefficient for barotropic pressure-driven currents. *J. Phys. Oceanogr.*, (in press).
- Mofjeld, H.O., and J.W. Lavelle, 1984. Setting the length scale in a second-order closure model of the unstratified bottom boundary layer. *J. Phys. Oceanogr.*, *14*, 834-839.
- Nezu, I., and W. Rodi, 1986. Open-channel flow measurements with a laser Doppler anemometer. *J. Hydraul. Eng.*, *112*, 335-355.
- Richards, K.J., 1982. Modeling the benthic boundary layer. *J. Phys. Oceanogr.*, *12*, 428-439.
- Rodi, W., 1980. Turbulence models and their application in hydraulics. IAHR-Section on Fundamentals of Division II: Experimental and Mathematical Fluid Dynamics, Delft, The Netherlands, 104 pp.

- Rouse, H., 1937. Modern conceptions of the mechanics of fluid turbulence. *Trans. A.S.C.E.*, 102, 463-543.
- Rouse, H., 1961. *Fluid Mechanics for Hydraulic Engineers*. Dover, New York, 422 pp.
- Schlichting, H., 1979. *Boundary-Layer Theory*. McGraw-Hill, New York, 817 pp.
- Sleath, J.F.A., 1984. *Sea Bed Mechanics*. John Wiley and Sons, New York, 335 pp.
- Vanoni, V.A., 1946. Transportation of suspended sediment by water. *Trans. A.S.C.E.*, 111, 67-133.
- Vanoni, V.A., 1984. Fifty years of sedimentation. *J. Hydraul. Eng.*, 110, 1021-1057.
- van Rijn, L.C., 1984. Sediment transport. Part II: Suspended load transport. *J. Hydraul. Eng.*, 110, 1613-1641.
- Weatherly, G.L., and P.J. Martin, 1978. On the structure and dynamics of the oceanic bottom boundary layer. *J. Phys. Oceanogr.*, 8, 557-570.

## Errata

Table 2:  $H' = 1.00$  should be  $H' = 1.00H$

Eq. 26:  $\dots (1-Z)^\beta dz$  should be  $\dots (1-Z)^\beta dZ$

Table 3:  $H' = 1.07$  should be  $H' = 1.07H$

Eq. 27:  $F = \frac{E H}{\kappa^2 \beta} \left[ \frac{Z_o}{1-Z_o} \right]^\beta \left\{ \dots \right.$  should be  $F = \frac{E H}{\kappa^2 \beta} \left\{ \left[ \frac{Z_o}{1-Z_o} \right]^\beta \dots \right.$

Table 5:  $\dots$  (27) in the formula (26)  $\dots$  should be  $\dots$  (29) in the formula (28)  $\dots$

Eq. 32:  $F = \frac{E H}{\kappa^2 \beta} \left[ \dots \right.$  should be  $F = \frac{E H}{\kappa^2 \beta} \left[ \frac{z_o}{H-z_o} \right] \left[ \dots \right.$